

Received: 2018.01.23
Accepted: 2018.03.08
Published: 2018.03.23

Highly Expressed Granulocyte Colony-Stimulating Factor (G-CSF) and Granulocyte Colony-Stimulating Factor Receptor (G-CSFR) in Human Gastric Cancer Leads to Poor Survival

Authors' Contribution:
Study Design A
Data Collection B
Statistical Analysis C
Data Interpretation D
Manuscript Preparation E
Literature Search F
Funds Collection G

ABCDEF 1 **Zhisong Fan**
ABCDEF 2 **Yong Li**
BC 2 **Qun Zhao**
ABC 2 **Liqiao Fan**
CDE 2 **Bibo Tan**
EF 1 **Jing Zuo**
ABCE 2 **Kelei Hua**
BCE 2 **Qiang Ji**

1 Department of Oncology, The Fourth Hospital of Hebei Medical University, Shijiazhuang, Hebei, P.R. China
2 Third Department of Surgery, The Fourth Hospital of Hebei Medical University, Shijiazhuang, Hebei, P.R. China

Corresponding Author: Yong Li, e-mail: li_yong_hbth@126.com

Source of support: This work is supported by grants from Youth Science and Technology Project (No. 20150810) of Hebei Province Health and Family Planning Commission

Background: Chemotherapy for advanced gastric cancer (GC) patients has been the mainstay of therapy for many years. Although adding anti-angiogenic drugs to chemotherapy improves patient survival slightly, identifying anti-angiogenic therapy-sensitive patients remains challenging for oncologists. Granulocyte colony-stimulating factor (G-CSF) promotes tumor growth and angiogenesis, which can be minimized with the anti-G-CSF antibody. Thus, G-CSF might be a potential tumor marker. However, the effects of G-CSF and G-CSFR expression on GC patient survival remain unclear.

Material/Methods: Seventy GC tissue samples were collected for G-CSF and G-CSFR detection by immunohistochemistry. A total of 40 paired GC tissues and matched adjacent mucosa were used to measure the G-CSF and G-CSFR levels by ELISA. Correlations between G-CSF/G-CSFR and clinical characteristics, VEGF-A levels and overall survival were analyzed. Biological function and underlying mechanistic investigations were carried out using SGC7901 cell lines, and the effects of G-CSF on tumor proliferation, migration, and tube formation were examined.

Results: The levels of G-CSFR were upregulated in GC tissues compared to normal mucosa tissues. Higher G-CSF expression was associated with later tumor stages and higher tumor VEGF-A and serum CA724 levels, whereas higher G-CSFR expression was associated with lymph node metastasis. Patients with higher G-CSF expression had shorter overall survival times. *In vitro*, G-CSF stimulated SGC7901 proliferation and migration through the JAK2/STAT3 pathway and accelerated HUVEC tube formation.

Conclusions: These data suggest that increased G-CSF and G-CSFR in tumors leads to unfavorable outcomes for GC patients by stimulating tumor proliferation, migration, and angiogenesis, indicating that these factors are potential tumor targets for cancer treatment.

MeSH Keywords: **Angiogenesis Inducing Agents • Granulocyte Colony-Stimulating Factor • Receptors, Granulocyte Colony-Stimulating Factor • Stomach Neoplasms • Survival • Vascular Endothelial Growth Factor A**

Full-text PDF: <https://www.medscimonit.com/abstract/index/idArt/909128>

 3624  2  5  25



Background

Gastric cancer (GC) is the second most prevalent cancer and the third leading cause of cancer-related death in China. The incidence of GC was 30.77/100,000 in 2010, accounting for 13.08% of all cancers in China [1]. Although targeted therapy and immunotherapy have developed rapidly, chemotherapy is still the most effective treatment for advanced GC patients.

Angiogenesis plays an important role in the development of cancer. Vascular endothelial growth factor (VEGF), a key factor in the angiogenesis process, promotes tumor survival, migration, and invasion. Bevacizumab is the first FDA-approved anti-angiogenic agent and takes effect by specifically binding to VEGF-A. Although bevacizumab is associated with significantly longer progression-free survival and a higher overall response rate versus placebo, the difference in overall survival (OS) is not statistically significant [2]. Further evaluation has found that plasma VEGF-A is a biomarker candidate for predicting the clinical outcomes of patients with advanced GC treated with bevacizumab [3]. Most recently, the anti-VEGF receptor 2 drug ramucirumab has been reported to improve survival both as a single agent relative to best supportive care and as a combination therapy with paclitaxel relative to paclitaxel alone in pretreated patients [4,5]. The addition of anti-angiogenic drugs to chemotherapy is a promising approach, even though the improvement in survival is small. However, identifying anti-angiogenic therapy-sensitive patients remains challenging for oncologists.

By binding to granulocyte colony-stimulating factor (G-CSF) receptor (G-CSFR), G-CSF stimulates granulocyte production and neutrophil differentiation and mobilization [6]. Recombinant human G-CSF (rhG-CSF) is widely used for chemotherapy-induced leukopenia. Recent studies *in vitro* have demonstrated that G-CSF can be produced by carcinoma cells and tumor stromal myofibroblasts [7]. Moreover, G-CSF may induce tumor proliferation, migration, and angiogenesis [8–10]. In many cases, G-CSF-producing tumors are detected at an advanced stage and are associated with a poor prognosis [11,12]. G-CSF expression has shown a strong correlation with resistance to anti-VEGF treatment [13]. Treatment with anti-G-CSF monoclonal antibody results in reduced tumor angiogenesis and growth [13]. Thus, G-CSF might be a potential biomarker for prognosis and anti-angiogenic drug efficacy. However, the mechanism underlying the effects of G-CSF on GC development remain to be elucidated.

To explore the role of G-CSF and G-CSFR in GC development, we examined the expression levels of G-CSF and G-CSFR in cancer and adjacent mucosa tissues and investigated the associations with clinicopathology, VEGF-A expression, and patient survival. In addition, we elucidated the effects of G-CSF on GC *in vitro*.

Material and Methods

Human samples

Paraffin-embedded cancer samples from 70 GC patients were collected in the Fourth Hospital of Hebei Medical University. These patients underwent surgery from August 2013 to December 2013. Another group of GC samples and adjacent mucosa (at least 5 cm away from the edge of tumor) samples from an additional 40 patients diagnosed with GC was collected from April–August 2014 in the same hospital. None of these patients had received chemotherapy or radiotherapy before surgical tumor resection. Follow-up data were obtained by phone.

Fresh tissues were collected immediately after surgical removal, frozen in liquid nitrogen, and stored at -80°C .

The histomorphology of the specimens was confirmed by the Department of Pathology at the same hospital. Staging procedures included physical examinations, blood tests, and chest and abdominal computed tomography (CT). Radioisotopic bone scans and brain CT scans were also performed when necessary. Tumor-node-metastasis (TNM) staging was based on surgical and histological findings, according to the American Joint Committee on Cancer (AJCC) 7th edition.

Immunohistochemistry

Streptavidin-peroxidase immunohistochemistry was used to detect the expression of G-CSF, G-CSFR, and VEGF-A in 4- μm thick paraffin-embedded tissues. High temperature and the pressure antigen retrieval method with citrate antigen retrieval buffer were used for antigen retrieval. Sections were incubated with anti-G-CSF (1: 15, BIOBASIC, China), anti-G-CSFR (1: 15, BIOBASIC, China), and anti-VEGF-A (1: 50, BIOS, China) polyclonal rabbit antibodies or with PBS instead of a primary antibody as the negative control for 60 min at room temperature. Then, the PBS solution was removed, 50 μL of MaxVisionTM2 reagent was added dropwise to the sections, and the sections were incubated at room temperature for 15 min. The PBS solution was removed, and the sections were stained with diaminobenzidine.

Enzyme-linked immunosorbent assay

The concentrations of G-CSF, G-CSFR, and VEGF-A in the tissue homogenates were measured with ELISA kits (BLUE GENE, China) according to the manufacturer's instructions. All experiments were performed in triplicate.

Cell lines and cell culture

Gastric cell lines (including AGS, MGC-803, BGC-823, and SGC-7901) were cultured. As SGC-7901 had the highest G-CSFR expression (data not shown), this cell line was chosen for subsequent studies. SGC7901 cells were cultured in RPMI 1640 with 10% fetal bovine serum (HyClone, USA) and maintained in a humidified atmosphere with 5% CO₂ at 37°C. Human umbilical vein endothelial cells (HUVECs) were obtained from ScienCell and maintained in Endothelial Cell Medium (ScienCell, no. 1001). Prior to stimulation with G-CSF, cells were incubated in serum-free medium for 24 hours.

Western blotting

Cells were lysed in RIPA lysis buffer (Solarbio, China), and the lysates were harvested by centrifugation at 12 000 rpm for 15 min at 4°C. Protein concentrations were determined with bicinchoninic acid (BCA) protein assays (Thermo, USA). Equal amounts of protein were electrophoresed on 10% SDS-PAGE gels and transferred onto PVDF membranes (Millipore, MA, USA). Membranes were blocked with 5% dry milk in TTBS for 2 hours at room temperature and incubated overnight at 4°C with primary antibodies. The membranes were then incubated with secondary antibody at room temperature for 1 hour, and the Odyssey 2-color infrared fluorescence scanning system (LI-COR, Biosciences, USA) was used for imaging and analysis.

Real-time (RT) PCR

Total RNA was extracted with TRIzol (Invitrogen, USA), and 1 µg of RNA was subjected to reverse transcription using a first-strand cDNA synthesis kit (Promega, USA) according to the manufacturer's instructions. Real-time PCR analysis was performed with the ABI 7500 FAST system, using the Platinum A6001 GoTaq[®]qRT-PCR Master Mix Kit (Promega, USA), according to the manufacturer's instructions. To amplify the G-CSFR transcripts, we used the primer pairs 5'-ATAAGTTTGTCTCTTTTACA-3' (sense) and 5'-GGAGTTCTGTCTGACC-3' (antisense). The 2^{-ΔΔCT} method was applied to analyze the relative mRNA expression levels.

Cell proliferation assay

Cell proliferation assays were performed with the Cell Counting Kit-8 (CCK-8; Dojindo, Kumamoto, Japan) assay according to the manufacturer's recommendations. After incubations of SGC7901 cells with rhG-CSF at various concentrations (0, 10, 50, and 100 ng/mL) for different times (24, 48, 72, and 96 hour), CCK-8 solution was added (10 µL/well) to the cells, and the cells were incubated for 2 hours at 37°C. The absorbance was measured at 450 nm to quantify the relative cell density. All groups were evaluated with a minimum of 4 separate wells per experiment.

Wound healing assay

Cells (5×10⁵) were seeded in 24-well plates. When the cell confluence reached above 80%, scratch-wounds were made by scraping the cell layer with the tip of a 200-µL pipette. Cells were washed with PBS and incubated with 0 or 50 ng/mL rhG-CSF. Phase-contrast microscopic images were obtained at 0, 12, and 24 hours after incubation, and the migration distance was measured. The experiments were performed in triplicate.

Transwell invasion assay

Transwell invasion assays were performed using 24-well Transwell plates (Corning Costar, USA). The 24-well plates with 8.0-µm pores were coated with Matrigel (BD Biosciences, USA). SGC7901 cells were seeded into the upper membrane chambers at a density of 1 × 10⁵/mL in serum-free medium with or without rhG-CSF (50 ng/mL), and 600 µL of medium containing 10% FBS was added to each lower chamber. After incubation for 20 hours, cells adhering to the upper surfaces of the membranes were removed with a cotton swab. The migrated cells, which adhered to the lower surfaces, were stained with crystal violet. The numbers of migrated cells were determined from 5 randomly chosen fields under an inverted microscope. Data were obtained from 3 independent experiments.

Tube formation assay

Matrigel solution was thawed overnight at 4°C, and all plasticware was precooled at -20°C. HUVECs that were resuspended in Endothelial Cell Medium with rhG-CSF at 0 ng/mL, 10 ng/mL, 50 ng/mL and 100 ng/mL were seeded onto growth factor-reduced Matrigel (250 µL/well) in a 24-well tissue culture-treated plate. The 24-well plate was incubated at 37°C in 5% CO₂ for 12 hours. Images were obtained with randomly chosen fields in each well at 100x magnification. For quantitative analysis, the length of endothelial network formation in each image was calculated with Image-Pro Plus 6.0 (Media Cybernetics, Inc., USA). All experiments were performed in quadruplicate, and the data are expressed as the length of the network (mean length/field).

Statistical analysis

All statistical analyses were performed using SPSS 21.0 software. Correlations of protein expression with immunohistochemistry and clinicopathologic parameters were evaluated with χ^2 tests or Fisher's exact probability tests. The expression levels of indicated factors in the different groups were compared with the Mann-Whitney test or Kruskal-Wallis test. Cancer and normal tissues were compared as 2 related samples with the Wilcoxon signed-rank test. The Spearman rank correlation test was employed for correlation analysis. The

follow-up time was calculated from the date of surgery to the date of death or last known follow-up. Kaplan-Meier analysis was performed to evaluate survival. Statistically significant differences were defined as comparisons with $P \leq 0.05$.

Results

G-CSF and G-CSFR expression in human GC and adjacent mucosa

Although G-CSF and G-CSFR are reportedly expressed in various tumor cell types *in vitro* [7–9,14], the expression levels of G-CSF and G-CSFR in GC are unknown. Thus, immunohistochemistry was performed to detect the expression of G-CSF and G-CSFR in GC tissues collected from patients. The results showed that G-CSF and G-CSFR were expressed at the GC cell membrane and cytoplasm and in some tumor tissue-infiltrating lymphocytes (Figure 1A). A total of 85.7% (60 out of 70) of the cancer tissues showed strong G-CSFR staining, and 28.6% (20 out of 70) of the cancer tissues showed strong G-CSF staining. No negative expression was observed. There was a significant correlation between G-CSF and G-CSFR expression in the GC tissues ($P=0.031$).

Furthermore, we used ELISA to measure the expression levels of G-CSF and G-CSFR in pairs of tumor tissues and their matched adjacent normal mucosa from 40 patients. A total of 50% (20 out of 40) of the patients had higher G-CSF levels in their cancer tissues than in their normal mucosa tissues, and 65% (26 out of 40) of the patients had higher G-CSFR levels in their cancer tissue. The G-CSFR concentration (944.7 ± 1944.6 pg/mL) was significantly higher in the GC tissues than in the normal mucosa tissues (537.6 ± 273.6 pg/mL, $P=0.045$), whereas the G-CSF concentrations were not significantly different (cancer 182.5 ± 367.4 pg/mL vs. normal 119.1 ± 127.4 pg/mL) ($P=0.988$) (Figure 1B). The expression levels of G-CSF and G-CSFR were significantly correlated in both the cancer tissues and normal tissues ($P < 0.001$), which was consistent with the immunohistochemistry assessment, indicating cooperation between these 2 factors.

Correlation between G-CSF/G-CSFR expression and clinical pathology

To explore the expression of G-CSF and G-CSFR in tumors of different primary tumor (T), node (N), and metastasis (M) stages, we analyzed the G-CSF/G-CSFR expression intensity in tumors with different clinical pathologies.

In the immunohistochemistry analysis, G-CSF was significantly associated with TNM staging ($P=0.028$), while G-CSFR showed a strong association with lymph node metastasis ($P=0.018$) (Table 1). Although the concentrations of G-CSF and G-CSFR by ELISA were upregulated from stages I to III but unexpectedly

downregulated in stage IV, no obvious differences were evident among the different TNM stages (Figure 1C). Because patients with stage IV GC rarely undergo surgery, only 2 and 4 specimens were available for immunohistochemistry and ELISA, respectively, in our study. All of these patients had peritoneal metastases that were first discovered during surgery. Thus, whether G-CSF/G-CSFR really decreases in stage IV GC cancer tissues needs further exploration.

Tumor markers can be produced directly by tumor or non-tumor cells as a response to tumor presence. Sometimes the levels of the tumor markers are in accordance with the tumor burden. Therefore, we assessed the serum levels of CA724, CEA, CA199, and CA50 and found that the G-CSF levels in GC tissues were significantly correlated with the CA724 levels ($P=0.026$), indicating that serum CA724 may be a predictor of the G-CSF level in GC cancer tissue.

G-CSF and G-CSFR are predictors of poor survival for GC patients

The TNM staging system is often used to estimate patient survival. Because the G-CSF and G-CSFR levels were higher in the advanced TNM stage in our study, we hypothesized that G-CSF and G-CSFR could be used to estimate patient survival. To test this hypothesis, the 70 patients involved in our immunohistochemistry analysis were followed up for up to 4 years. The mortality rate of the patients with high G-CSF expression was significantly higher than that of the patients with low G-CSF expression (45% vs. 18%, $P=0.023$), and the same trend was evident for G-CSFR (30% vs. 0%, $P=0.04$). The 40 patients involved in the ELISA analysis were also monitored for up to 3 years. The G-CSF level was 376.9 ± 634.3 pg/mL in patients who had died and 117.7 ± 189.8 pg/mL in patients who had survived ($P=0.029$). The G-CSFR level was 1888.2 ± 3830.5 pg/mL in patients who had died and 630.2 ± 349.8 pg/mL in patients who had survived ($P=0.086$). The VEGF-A level was 40.6 ± 23.2 pg/mL in patients who had died and 29.6 ± 23.3 pg/mL in patients who had survived ($P=0.148$) (Figure 2A). Therefore, one can predict that patients with high G-CSF expression in their GC tissues may have unfavorable outcomes.

Consistent findings were observed by Kaplan-Meier analysis, which was used to evaluate the OS of the patients. The patients with high G-CSF in their GC tissue had significantly worse OS than the patients with low G-CSF ($P=0.006$) (Figure 2B). The results indicated that G-CSF expression in GC tissue is a predictor of poor prognosis.

G-CSF induces GC cell proliferation and migration

G-CSF correlation with TNM staging and OS suggests that G-CSF may promote tumor development. To explore the effect

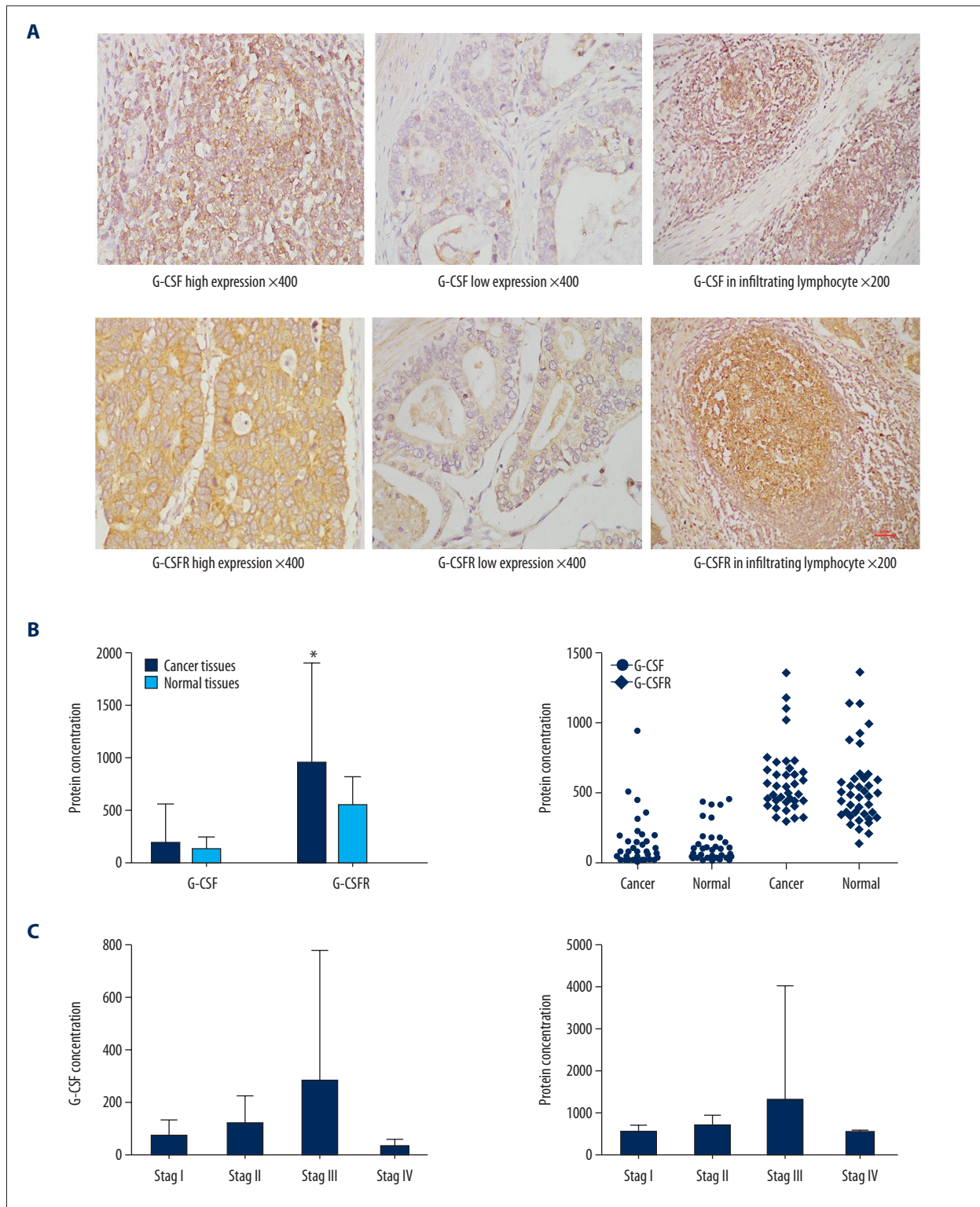


Figure 1. G-CSF and G-CSFR expression in GC tissues. **(A)** The expression of G-CSF and G-CSFR was detected in cancer cells and tumor-infiltrating lymphocytes by immunohistochemistry. **(B)** G-CSF and G-CSFR protein concentrations were measured in 40 paired (cancer and normal tissue) gastric tissues by ELISA, and the G-CSFR levels in the cancer tissues were significantly higher than those in the normal tissues ($P=0.045$). **(C)** G-CSF and G-CSFR protein levels at different TNM stages by ELISA. * $P<0.05$.

Table 1. Correlation between G-CSF/G-CSFR expression and clinicopathological parameters of 70 patients.

Clinical pathological parameters	G-CSF expression		χ^2	P	G-CSFR expression		χ^2	P
	Low	High			Low	High		
Gender								
Male	37	15	0.007	1.000	8	44	0.005	0.955
Female	13	5			2	16		
Age								
<60	23	12	1.120	0.428	5	30	0.000	1.000
≥60	27	8			5	30		
Lauren classification								
Intestinal	44	15	1.823	0.274	9	50	0.004	0.947
Diffuse	6	5			1	10		
Differentiation								
Poor	26	9	0.284	0.940	6	29	0.770	0.826
Moderate	15	7			3	19		
Well	11	4			1	12		
Invasion depth								
T1+T2	29	6	4.480	0.063	8	27	2.318	0.171
T3+T4	21	14			2	33		
Lymph node metastasis								
Negative	25	6	2.316	0.184	8	23	6.031	0.018
Positive	25	14			2	37		
TNM stage								
I+II	35	8	5.426	0.030	8	35	1.689	0.297
III+IV	15	12			2	25		

of G-CSF on cancer development, GC cells (SGC7901) were cultured, and Western blotting and CCK8 assays were performed to examine whether G-CSF could promote GC cell proliferation. As shown in Figure 3A, PCNA levels markedly increased in a dose-dependent manner in the GC cells after G-CSF treatment. CCK8 analysis also showed that G-CSF induced cell proliferation (Figure 3B).

Wound healing assays were performed to determine the effects of G-CSF on GC cell migration. As shown in Figure 3C, wound healing was significantly more rapid for the G-CSF-stimulated cells than for the untreated cells. Transwell migration assays were also performed and showed that G-CSF significantly promoted GC cell invasion (Figure 3D).

G-CSF induces proliferation and migration through JAK2/STAT3 signaling

To elucidate the molecular mechanisms of the G-CSF-induced SGC7901 cell proliferation and migration, further experiments were conducted to explore the signaling pathway through which G-CSF promoted cell proliferation and migration.

We examined several signaling pathways (data not shown) and found that G-CSF could induce activator of transcription (STAT)3 phosphorylation and upregulate Janus kinase (JAK)2 expression in SGC7901 cells (Figure 3E). To further determine whether the stimulation of phospho-STAT3 and JAK2 occurred due to G-CSF binding to G-CSFR, SGC7901 cells were incubated with an antibody against G-CSFR (1 µg/mL) for 6 hours and then stimulated with G-CSF, as described previously [8]. Figure 3E shows that G-CSF-induced phospho-STAT3 and JAK2

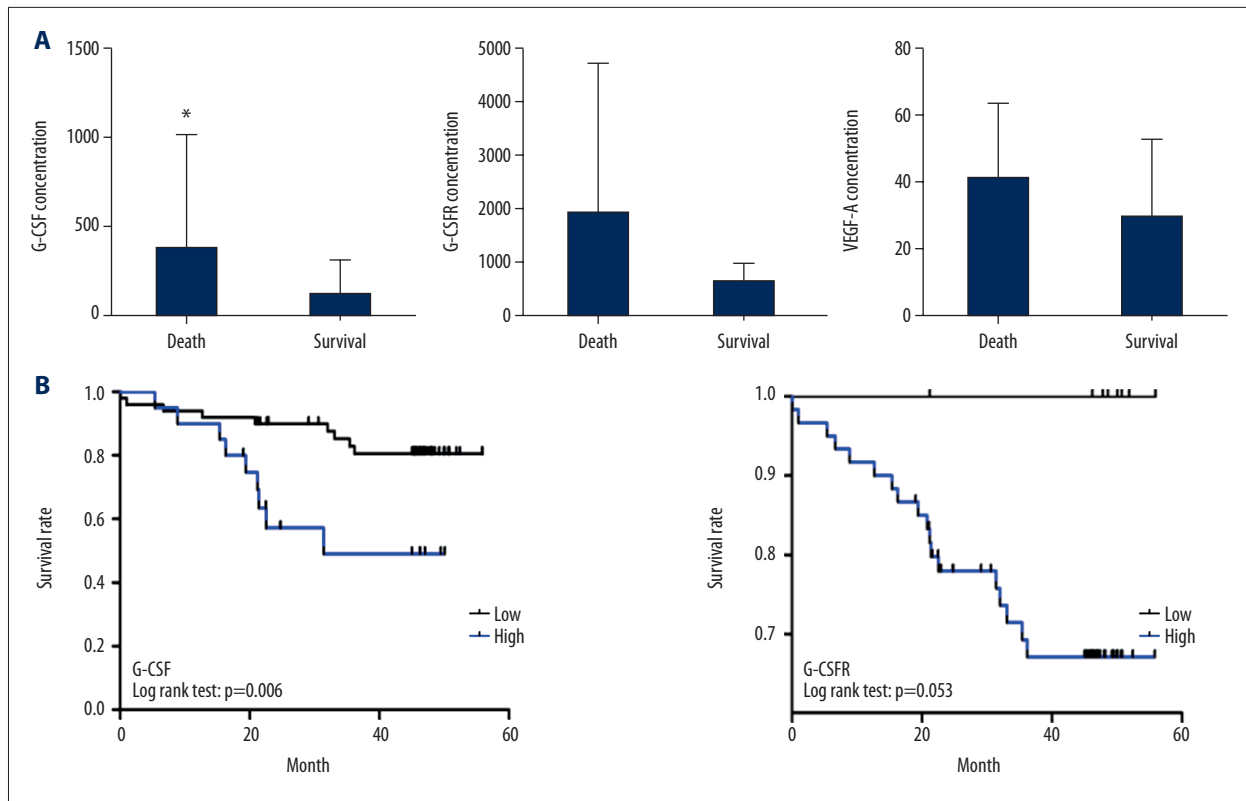


Figure 2. G-CSF/G-CSFR correlation with GC patient survival. (A) The concentrations of G-CSF, G-CSFR and VEGF-A were measured in patients who had died and those who survived by ELISA. The G-CSF concentration was significantly higher in patients who had died than in those who had survived. (B) Kaplan-Meier postoperative survival analysis of OS for GC (n=70) using immunohistochemistry. High G-CSF expression was associated with poor OS. * $P < 0.05$.

upregulation was inhibited by the anti-G-CSFR antibody. These data indicate that G-CSF may induce GC proliferation through the JAK2/STAT3 signaling pathway.

Exogenic G-CSF promotes G-CSFR expression

Because we found that G-CSF was strongly correlated with G-CSFR in GC tissues, we asked whether G-CSF could promote G-CSFR expression. After incubations of SGC7901 cells with G-CSF (50 ng/mL) for 96 hours, RT-PCR and Western blotting analyses showed that G-CSFR expression was dramatically up-regulated (Figure 4). This result suggested that exogenic G-CSF could stimulate G-CSFR expression in tumor cells. As G-CSFR contains 2 motifs (box1 and box2) that are essential for the activation of JAK2 [15], G-CSFR may be the intermediate factor between G-CSF and JAK2/STAT3 activation.

G-CSF promotes angiogenesis

Previous *in vitro* and *in vivo* analyses have shown that G-CSF can stimulate neutrophils to secrete VEGF, a factor that plays an important role in angiogenesis, and consequently promote angiogenesis [16]. Therefore, we performed experiments to

determine whether G-CSF was associated with VEGF-A expression and angiogenesis in GC tissues. From TNM stages I to IV, VEGF-A expression was upregulated, showed no significant differences among the different TNM stages (Figure 5A) and was strongly associated with G-CSFR ($P=0.001$) but not with G-CSF ($P=0.468$) (Figure 5B). The immunohistochemistry analysis showed that VEGF-A expression was also significantly associated with G-CSFR but not with G-CSF (Table 2). We subsequently found that G-CSF stimulation could not induce VEGF-A expression in SGC7901 cells (data not shown). These results indicated that G-CSFR upregulation was associated with increased VEGF-A expression in GC tissues, but VEGF-A expression was not stimulated directly by G-CSF in tumor cells.

To examine whether G-CSF could directly stimulate endothelial tubule formation *in vitro*, tube formation assays were performed. After incubations of HUVECs with G-CSF, tube formation was gradually enhanced in a concentration-dependent manner (Figure 5C). These results suggest that, in tumors, G-CSF can facilitate angiogenesis by promoting tube formation directly and VEGF-A expression indirectly.

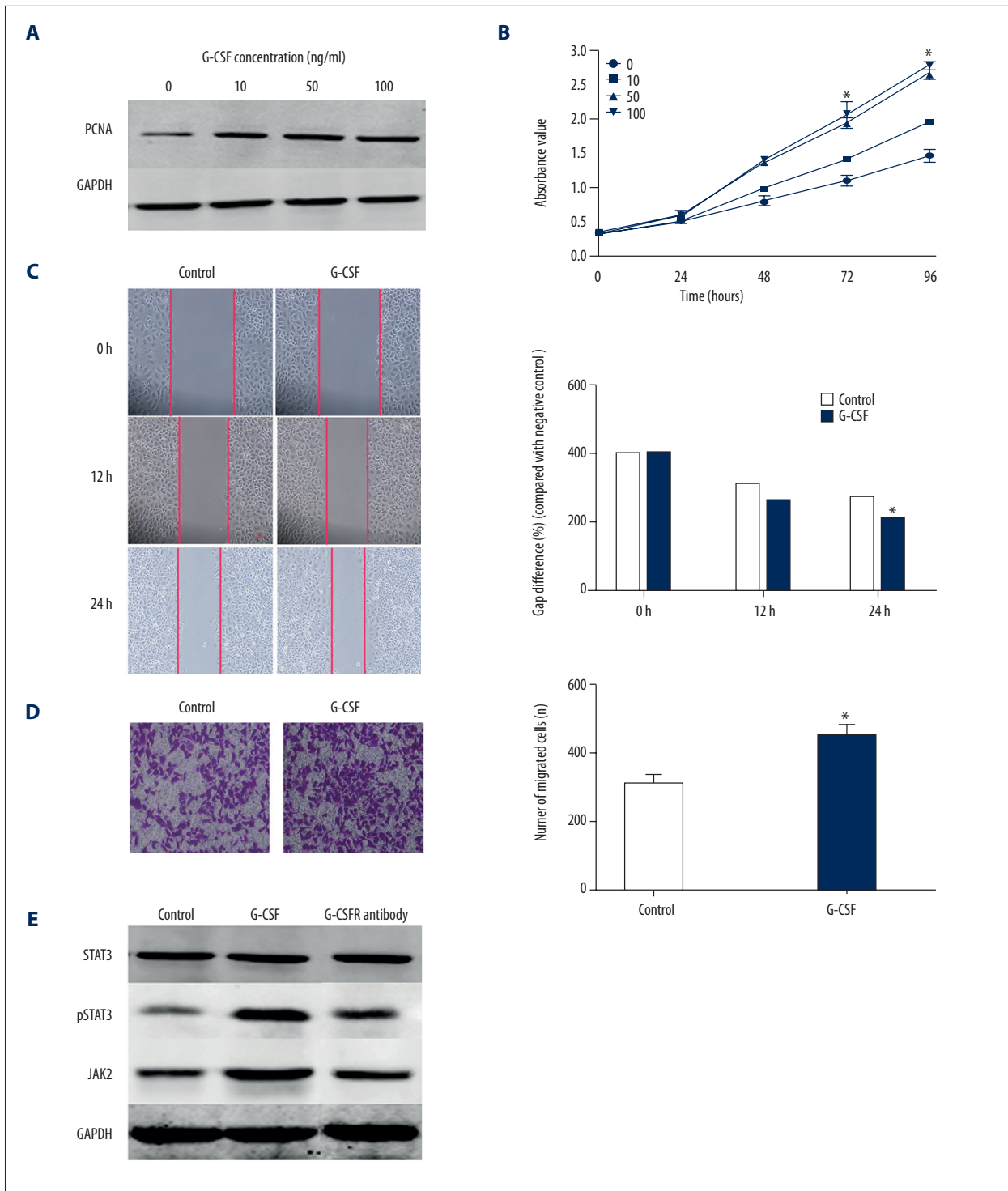


Figure 3. G-CSF promotes GC cell proliferation and migration via the JAK2/STAT3 pathway. **(A)** PCNA expression was detected in GC cells by Western blot. **(B)** GC cell proliferation with CCK8 assays. **(C)** G-CSF promotes GC cell migration in wound healing assays. **(D)** G-CSF promotes GC cell invasion in Transwell invasion assays. **(E)** The protein levels of STAT, phospho-STAT3 and JAK2 were examined by Western blotting with anti-STAT, anti-phospho-STAT3 and anti-JAK2 antibodies, respectively, in untreated (control) cells, in cells that were treated with G-CSF and in cells that were treated with anti-G-CSFR antibody before incubation with G-CSF. The expression levels of phospho-STAT3 and JAK2 were significantly increased in the G-CSF group compared to the control group and anti-G-CSFR group. * $P < 0.05$.

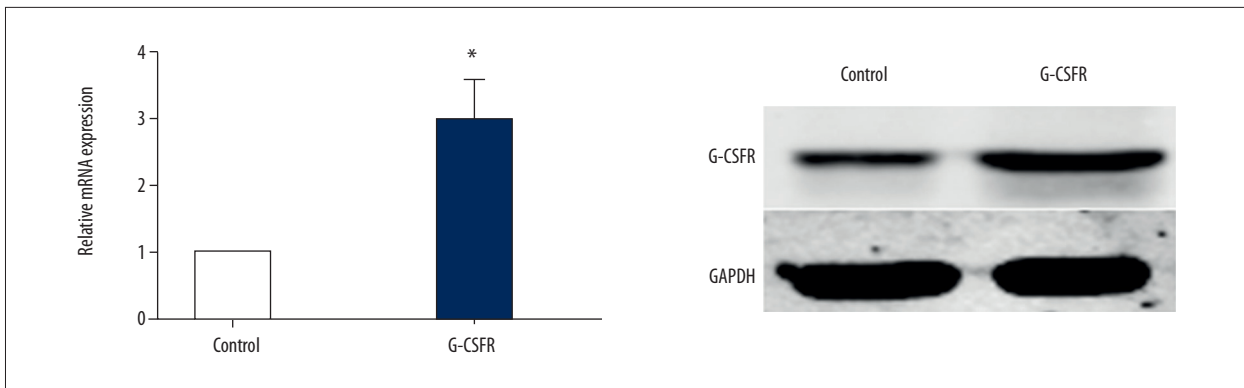


Figure 4. G-CSFR expression evaluation in GC cells by qRT-PCR and Western blotting with anti-G-CSFR antibody. Cells treated with G-CSF (50 ng/mL) for 96 hours have significantly higher G-CSFR mRNA and protein levels than untreated (control) cells. * $P < 0.05$ vs. control.

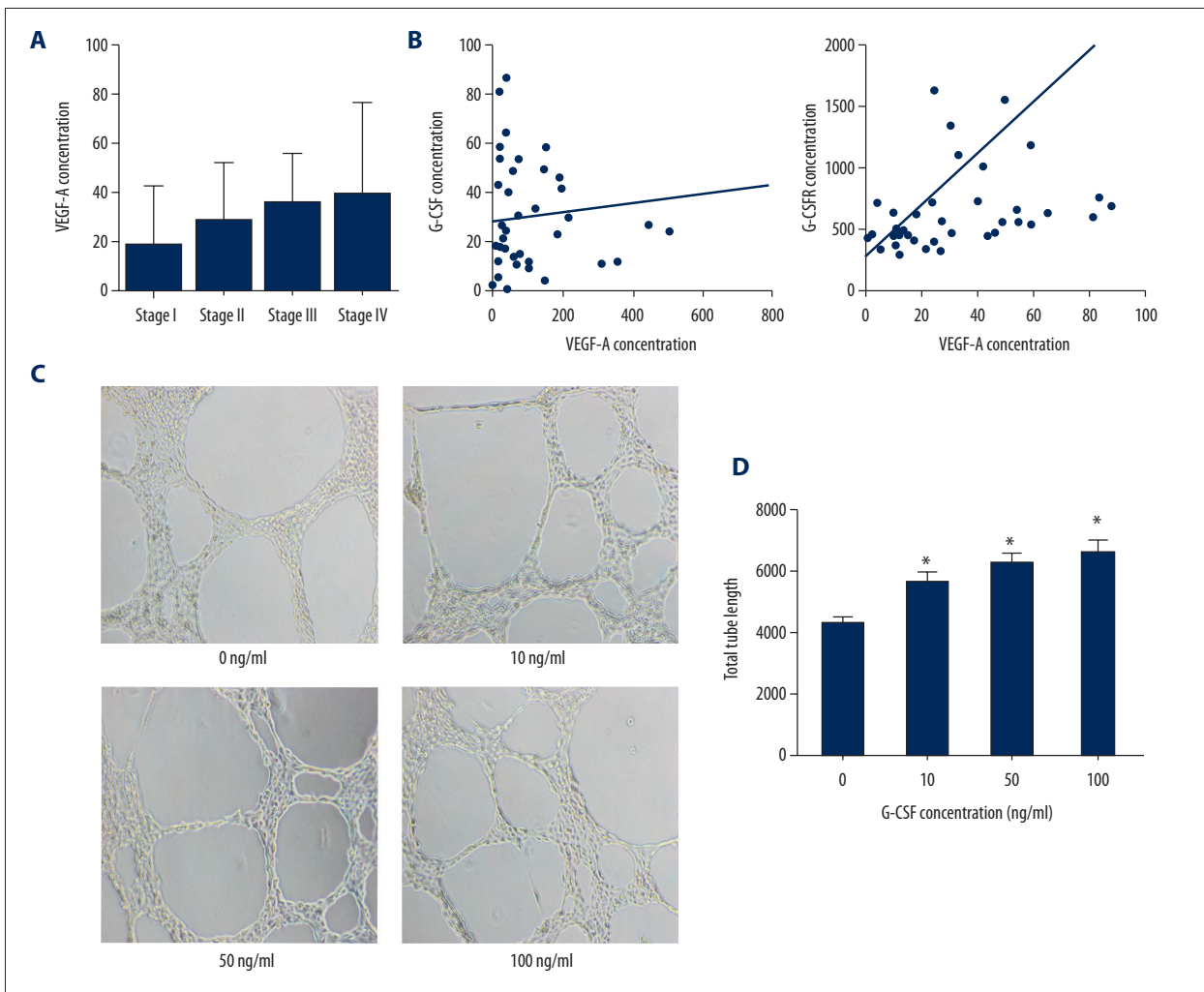


Figure 5. G-CSF promotes angiogenesis. (A) The VEGF-A protein concentrations for different TNM stages by ELISA. (B) The correlations of protein concentration between G-CSF/G-CSFR and VEGF-A. VEGF-A was significantly correlated with G-CSFR in GC tissues ($P = 0.001$). (C) HUVEC network formation on matrix gel. G-CSF stimulated HUVEC network formation in a dose-dependent manner. (D) The total tube length was quantified. G-CSF (10, 50, and 100 ng/mL) significantly promoted tube formation compared to the control group. * $P < 0.05$ vs. control.

Table 2. Correlation between G-CSF/G-CSFR and VEGF.

	VEGF expression		χ^2	P
	Low	High		
G-CSF				
Low	20	30	1.40	0.28
High	5	15		
G-CSFR				
Low	8	2	9.966	0.003
High	11	43		

Taken together, our results indicate that G-CSF can promote GC cell proliferation and migration through the JAK2/STAT3 signaling pathway and stimulate angiogenesis, which may lead to the poor survival of GC patients.

Discussion

G-CSF is a glycoprotein that stimulates bone marrow to produce granulocytes and stem cells and release them into the bloodstream. G-CSF also stimulates the survival, proliferation, and differentiation of neutrophil precursors and mature neutrophils. G-CSFR, which belongs to the class I cytokine (or hematopoietin) receptor superfamily, is a single transmembrane protein and a cell-surface receptor for the G-CSF [15]. Studies over the past decade have focused on the different functions of G-CSF/G-CSFR, such as tumor growth, angiogenesis and pain alleviation [7,10,13,17]. G-CSF/G-CSFR expression has been detected in many kinds of malignant tumors, such as ovarian, uterine, cervical, and colorectal cancers and glioma [7–9,12]. In our study, G-CSF/G-CSFR expression was widely detected in GC tissues and normal gastric mucosa. The protein levels of G-CSF and G-CSFR were upregulated from stage I to III but downregulated in stage IV. This result was similar to that observed in the study by Morris KT et al., in which stage III samples exhibited significantly higher mRNA expression of G-CSF and G-CSFR than did stage II and IV samples [7]. Whether this change is due to cancer development or due to the small sample size requires further study.

rhG-CSF is widely used to accelerate recovery from neutropenia after chemotherapy. As shown in this study, rhG-CSF can upregulate G-CSFR, which is significantly correlated with lymph node metastasis. Thus, further investigations are needed to determine whether the current practice of using rhG-CSF after chemotherapy reduces drug effects by upregulating tumor G-CSFR and promoting G-CSFR-positive tumor development.

Following GC worsening, G-CSF/G-CSFR expression is upregulated. GC patients with high G-CSF expression have shorter

OS times, indicating that G-CSF is a potential predictor of poor prognosis for GC. As the receptor of G-CSF, G-CSFR stimulates numerous signal transduction proteins, including JAK/STAT, mitogen-activated protein kinases (MAPKs), and serine/threonine kinases (Akt) [18]. The JAK2/STAT3 pathway stimulated by G-CSF is the most studied pathway in tumor cells. G-CSF can induce STAT3 phosphorylation, which can be inhibited by either an antibody against phospho-STAT3 and a JAK2 inhibitor [9] or an antibody against G-CSFR [8]. The proliferation of different human neuroblastoma cell lines can be markedly inhibited by low levels of STAT3 dimerization inhibitor, and G-CSF-positive cells are more sensitive to this inhibition than are G-CSF-negative cells [19]. Inhibiting phospho-STAT3 or JAK2 can block the G-CSF-induced migration of ovarian cancer cells [9]. We found that by binding to G-CSFR, G-CSF stimulated STAT3 phosphorylation and JAK2 upregulation, which might promote GC cell proliferation and migration. G-CSFR expression showed a strong correlation with lymph node metastasis, indicating that G-CSFR upregulation may promote cancer metastasis.

Angiogenesis plays an important role in tumor survival and metastasis. G-CSF can improve the mobilization and angiogenesis of endothelial progenitor cells by stimulating VEGF secretion from neutrophils [16]. Anti-VEGF therapy combined with anti-G-CSF therapy can reduce tumor growth compared with anti-VEGF monotherapy [13]. In our study, G-CSFR was strongly associated with VEGF-A expression in GC tissues. VEGF-A can intensely promote HUVEC proliferation, migration, and endothelial network formation [20,21]. Therefore, G-CSFR upregulation in cancer tissues may promote angiogenesis by stimulating VEGF-A secretion. Although G-CSF could not directly induce VEGF-A secretion in GC cells (data not shown), we found that G-CSF still promoted endothelial network formation. Therefore, G-CSF and G-CSFR may play important roles in tumor angiogenesis.

The addition of anti-angiogenic drugs to chemotherapy shows some survival benefit for GC patients, but the efficacy of this approach is limited [2,4,5]. Methods for identifying patients who would benefit from the combination treatment need to

be explored. G-CSF can promote tumor angiogenesis and reduce the effects of anti-VEGF treatment in tumors [13]. High G-CSF levels in GC tissues may predict resistance to anti-angiogenic therapy. In our study, the tissue levels of G-CSF were significantly associated with the serum levels of CA724, the concentration of which in GC is usually used to evaluate disease severity and treatment effects [22–25]. Because serum CA724 is easily obtained, CA724 may be a candidate predictor of the efficacy of anti-angiogenic therapy for GC.

Conclusions

In summary, G-CSF accelerates GC development by promoting cell proliferation, migration, and angiogenesis through the

JAK2/STAT3 signaling pathway, ultimately leading to worse survival outcomes for patients. Considering that rhG-CSF is frequently used after chemotherapy, whether this treatment contributes to tumor development by increasing proliferation, migration, and angiogenesis, thereby shortening the survival time of patients, requires further study.

Acknowledgements

We would like to thank Cheng Yuan and Ming He, for reviewing the article and providing helpful advice.

Conflicts of interest

None.

References:

1. Zheng ZX, Zheng RS, Zheng SW, Chen WQ: [An analysis of incidence and mortality of stomach cancer in China, 2010.] *China Cancer*, 2014; 23: 795–800 [in Chinese]
2. Ohtsu A, Shah MA, Van Cutsem E et al: Bevacizumab in combination with chemotherapy as first-line therapy in advanced gastric cancer: A randomized double-blind placebo-controlled phase III study. *J Clin Oncol*, 2011; 29: 3968–76
3. Van Cutsem E, de Haas S, Kang YK et al: Bevacizumab in combination with chemotherapy as first-line therapy in advanced gastric cancer: A biomarker evaluation from the AVAGAST randomized phase III trial. *J Clin Oncol*, 2012; 30: 2119–27
4. Fuchs CS, Tomasek J, Yong CJ et al: Ramucirumab monotherapy for previously treated advanced gastric or gastro-oesophageal junction adenocarcinoma (REGARD): An international, randomised, multicentre, placebo-controlled, phase 3 trial. *Lancet*, 2014; 383: 31–39
5. Wilke H, Muro K, Van Cutsem E et al: Ramucirumab plus paclitaxel versus placebo plus paclitaxel in patients with previously treated advanced gastric or gastro-oesophageal junction adenocarcinoma (RAINBOW): A double-blind, randomised phase 3 trial. *Lancet Oncol*, 2014; 15: 1224–35
6. Demetri GD, Griffin JD: Granulocyte colony-stimulating factor and its receptor. *Blood*, 1991; 78: 2791–808
7. Morris KT, Khan H, Ahmad A et al: G-CSF and G-CSFR are highly expressed in human gastric and colon cancers and promote carcinoma cell proliferation and migration. *Br J Cancer*, 2014; 110: 1211–20
8. Wang J, Yao L, Zhao S et al: Granulocyte-colony stimulating factor promotes proliferation, migration and invasion in glioma cells. *Cancer Biol Ther*, 2012; 13: 389–400
9. Kumar J, Fraser FW, Riley C et al: Granulocyte colony-stimulating factor receptor signalling via Janus kinase 2/signal transducer and activator of transcription 3 in ovarian cancer. *Br J Cancer*, 2014; 110: 133–45
10. Okazaki T, Ebihara S, Asada M et al: Granulocyte colony-stimulating factor promotes tumor angiogenesis via increasing circulating endothelial progenitor cells and Gr1+CD11b+ cells in cancer animal models. *Int Immunol*, 2006; 18: 1–9
11. Yamano T, Morii E, Ikeda J, Aozasa K: Granulocyte colony-stimulating factor production and rapid progression of gastric cancer after histological change in the tumor. *Jpn J Clin Oncol*, 2007; 37: 793–96
12. Kawano M, Mabuchi S, Matsumoto Y et al: The significance of G-CSF expression and myeloid-derived suppressor cells in the chemoresistance of uterine cervical cancer. *Sci Rep*, 2015; 5: 18217
13. Shojaei F, Wu X, Qu X et al: G-CSF-initiated myeloid cell mobilization and angiogenesis mediate tumor refractoriness to anti-VEGF therapy in mouse models. *Proc Natl Acad Sci USA*, 2009; 106: 6742–47
14. Moon HW, Kim TY, Oh BR et al: Effects of granulocyte-colony stimulating factor and the expression of its receptor on various malignant cells. *Korean J Hematol*, 2012; 47: 219–24
15. Liongue C, Wright C, Russell AP, Ward AC: Granulocyte colony-stimulating factor receptor: Stimulating granulopoiesis and much more. *Int J Biochem Cell Biol*, 2009; 41: 2372–75
16. Ohki Y, Heissig B, Sato Y et al: Granulocyte colony-stimulating factor promotes neovascularization by releasing vascular endothelial growth factor from neutrophils. *FASEB J*, 2005; 19: 2005–7
17. Chao PK, Lu KT, Lee YL et al: Early systemic granulocyte-colony stimulating factor treatment attenuates neuropathic pain after peripheral nerve injury. *PLoS One*, 2012; 7: e43680
18. Panopoulos AD, Watowich SS: Granulocyte colony-stimulating factor: Molecular mechanisms of action during steady state and 'emergency' hematopoiesis. *Cytokine*, 2008; 42: 277–88
19. Agarwal S, Lakoma A, Chen Z et al: G-CSF promotes neuroblastoma tumorigenicity and metastasis via STAT3-dependent cancer stem cell activation. *Cancer Res*, 2015; 75: 2566–79
20. Bussolino F, Ziche M, Wang JM et al: *In vitro* and *in vivo* activation of endothelial cells by colony-stimulating factors. *J Clin Invest*, 1991; 87: 986–95
21. Lee M, Aoki M, Kondo T et al: Therapeutic angiogenesis with intramuscular injection of low-dose recombinant granulocyte-colony stimulating factor. *Arterioscler Thromb Vasc Biol*, 2005; 25: 2535–41
22. Li F, Li S, Wei L et al: The correlation between preoperative serum tumor markers and lymph node metastasis in gastric cancer patients undergoing curative treatment. *Biomarkers*, 2013; 18: 632–37
23. Emoto S, Ishigami H, Yamashita H et al: Clinical significance of CA125 and CA72-4 in gastric cancer with peritoneal dissemination. *Gastric Cancer*, 2012; 15: 154–61
24. Liu X, Cai H, Wang Y: Prognostic significance of tumour markers in Chinese patients with gastric cancer. *ANZ J Surg*, 2014; 84: 448–53
25. Zou L, Qian J: Decline of serum CA724 as a probable predictive factor for tumor response during chemotherapy of advanced gastric carcinoma. *Chin J Cancer Res*, 2014; 26: 404–9